

---

# Identifiability Challenges in Sparse Linear Ordinary Differential Equations

---

Cecilia Casolo, Sören Becker, Niki Kilbertus  
 Technical University of Munich  
 Helmholtz Munich  
 Munich Center for Machine Learning (MCML)  
 first.last@helmholtz-munich.de

## Abstract

Dynamical systems modeling is a core pillar of scientific inquiry across natural and life sciences. Increasingly, dynamical system models are learned from data, rendering identifiability a paramount concept. For systems that are not identifiable from data, no guarantees can be given about their behavior under new conditions and inputs, or about possible control mechanisms to steer the system. It is known in the community that “linear ordinary differential equations (ODE) are almost surely identifiable from a single trajectory.” However, this only holds for dense matrices. The sparse regime remains underexplored, despite its practical relevance with sparsity arising naturally in many biological, social, and physical systems. In this work, we address this gap by characterizing the identifiability of sparse linear ODEs. Contrary to the dense case, we show that sparse systems are unidentifiable with a positive probability in practically relevant sparsity regimes and provide lower bounds for this probability. We further study empirically how this theoretical unidentifiability manifests in state-of-the-art methods to estimate linear ODEs from data. Our results corroborate that sparse systems are also practically unidentifiable. Theoretical limitations are not resolved through inductive biases or optimization dynamics. Our findings call for rethinking what can be expected from data-driven dynamical system modeling and allows for quantitative assessments of how much to trust a learned linear ODE.

## 1 Introduction and related work

The field of dynamical systems has emerged early as a corner stone of scientific modeling, primarily due to the high demand for modeling temporally evolving systems in the natural and life sciences. For the most part, dynamical systems have been modeled “manually,” i.e., by humanly-prescribed differential equations or simulators inspired by, and validated in real-world systems. With the advent of machine learning and large data collection efforts, dynamical systems are increasingly learned from data. This new perspective also brought about a shift from an original focus on the *forward problem*—solving given differential equations from different initial conditions for predictions—to the *inverse problem*—finding the governing differential equation from observed trajectories. Learning the underlying dynamical laws simply from observing a system over time can be viewed as the ultimate goal of scientific discovery in many domains. A crucial pre-requisite for this goal becoming a reality is that the underlying law *can in principle be uniquely determined from the given observations*. If multiple different laws could result in the exact same observations, we are stuck. This is the problem of identifiability, as illustrated in Fig. 1: could the observed data have arisen from only a single unique dynamic? While solving the inverse problem poses a host of practical challenges, no guarantees can ever be given for the generalization capabilities of unidentifiable systems.

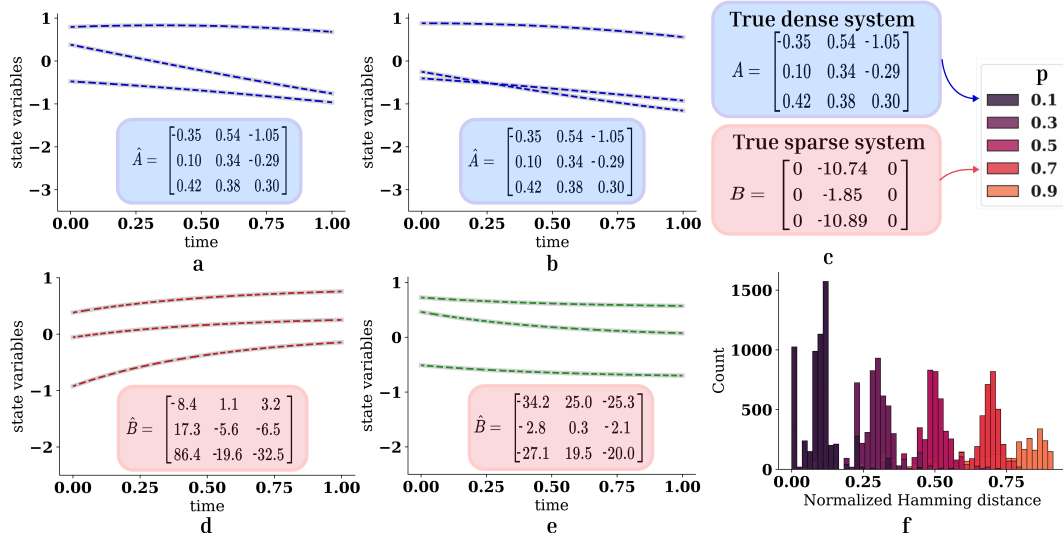


Figure 1: Identifiability differs between dense and sparse systems. The trajectories in **a** and **b** correspond to solutions for two different initial conditions of the dense system in **c**; similarly, trajectories in **d** and **e** correspond to solutions of the sparse system in **c**. All estimated trajectories (colored dashed curves) fit the respective observations (thick gray curves) well, yet only the estimate of the dense system is correct. The histogram in **f** shows that the normalized Hamming distance between the estimated and true system matrix systematically increases as sparsity  $p$  increases.

The identifiability of different types of dynamical systems from different types of observed data has been studied in a variety of domains like natural science [Donà et al., 2022, Muñoz-Tamayo et al., 2018], control theory [Ding and Toulis, 2020, Gargash and Mital, 1980], experimental design [Raue et al., 2010] and many more. Miao et al. [2011] provide a well-structured overview of how identifiability analysis of different types of (non-linear) dynamics is approached in practice while Scholl et al. [2022, 2023] have characterized necessary and sufficient conditions about what needs to be observed for identifiability in different functional classes of dynamics. The bio-mathematics community has been among the first to develop rigorous approaches to study identifiability [Bellman and Åström, 1970], referring to it as “structural identifiability.” Similarly, researchers in epidemiology have a strong track record in analyzing identifiability for domain-specific compartment models [Saccomani, 2011, Miao et al., 2011, Xia and Moog, 2003, Tuncer et al., 2016]. Cuniffe et al. [2024] recently analyzed the connection between identifiability and observability, as a critical aspect of epidemiological models, where we typically cannot observe the entire state. Stochastic differential equations often enjoy stronger theoretical identifiability guarantees, typically because the stochastic component is assumed to have full support, allowing to “probe the entire space” [Bellot et al., 2021, Wang et al., 2023].

Irrespective of theoretical considerations, new practical methods for learning dynamical systems from data are proposed continuously. These range from traditional parameter estimation techniques for ODEs [Lavielle et al., 2011, Commenges et al., 2011, Huang et al., 2006, Li et al., 2005, Brunton et al., 2016], to neural-network-based parameter estimation [Rubanova et al., 2019, Qin et al., 2019] as well as deep-learning based approaches that learn the dynamics as a neural net [Chen et al., 2018] or predicts symbolic expressions [Becker et al., 2023, d’Ascoli et al., 2024]. While these methods are reported to achieve strong *reconstruction performance*, i.e., they find dynamics that, when integrated from the same initial condition, recover the observed trajectories well, it is rarely reported to which extent they actually *identify the originally underlying dynamical law*. Due to unidentifiability, these methods could learn dynamical systems that do not generalize beyond the observed time spans or to new initial conditions, let alone warrant claims of scientific insights.

In this work, we will focus on linear, homogeneous, autonomous ordinary differential equations (ODE),  $\dot{x}(t) = Ax(t)$ , heavily relied upon in many domains while also amenable to rigorous theoretical analysis. Pioneering works by Stanhope et al. [2014] and, more recently, Qiu et al. [2022] established as a key result that “almost all such linear ODEs are identifiable from a single solution trajectory.” Here, it is assumed that we have observed the entire trajectory without any observation noise in continuous time. This is often paraphrased as “linear ODEs are identifiable” and summoned

by practitioners as justification to assume that whenever a linear ODE is estimated well from data, one has actually found the unique underlying governing law of the system with probability 1. The core contributions in this work build on the observation that this, rightfully celebrated, result only holds for dense matrices, i.e., they assume a measure over systems  $\mathbb{R}^{n \times n}$  that is absolutely continuous with respect to the  $n$ -dimensional Lebesgue measure  $\lambda^n$ .

This is not satisfied by sparse systems. Sparsity in dynamical systems means that not all variables depend on (or interact with) all other variables [Aliee et al., 2021], [Aliee et al., 2022]. Hence, sparsity allows us to understand and interpret complex networks pervasive in nature, society, and technology. In fact, dynamical models in biology [Lu et al., 2011] or social networks [Ravazzi et al., 2017] typically exhibit high degrees of sparsity. For example, Liben-Nowell [2005] asserts that “on average, a person has on the order of at most a thousand friends.” Similarly, interactions in gene regulatory networks are known to be sparse, with only a tiny fraction of possible pair-wise interactions being nonzero [Carey et al., 2018]. Hence, in many settings researchers only attempt to learn dynamical models from data when they assume interactions to be sparse, because meaningful interpretation is only possible in sparse models in the first place [Xu et al., 2023]. The resulting models are also believed to have a lower risk of overfitting, particularly when data is limited [Bartoldson et al., 2020].

**Contributions.** This work puts an asterisk on the result that “almost all linear ODEs are identifiable” proving positive lower bounds on the probability of *sparse systems* being unidentifiable. We also quantify theoretically to what extent “near unidentifiability” poses a challenge for practical identification in identifiable cases. Finally, we bridge the gap from theory to practice and demonstrate that (near) unidentifiability is not circumvented in practical methods by potential inductive biases or optimization dynamics. Our work clearly characterizes the regimes (in terms of dimensionality and sparsity) in which unidentifiability is an issue, and what observed time horizons are required to escape near unidentifiability.

## 2 Background and problem setting

We focus on autonomous, homogeneous, linear, noise-free ordinary differential equations (ODE), i.e., initial value problems (IVP) of the form

$$\dot{\mathbf{x}}(t) := \frac{d\mathbf{x}(t)}{dt} = A\mathbf{x}(t), \quad \mathbf{x}(0) = \mathbf{x}_0, \quad (1)$$

where  $A \in \mathbb{R}^{n \times n}$  is also called the *system* or simply referred to as the “ODE,”  $\mathbf{x} : [0, T] \rightarrow \mathbb{R}^n$  denotes the *trajectory*,  $\mathbf{x}_0 \in \mathbb{R}^n$  is the *initial condition*, and  $t$  denotes time. In autonomous systems, we can assume without loss of generality that the initial time is  $t = 0$  as autonomy implies that the system  $A$  is not time-dependent. Homogeneity ensures that the dynamics are not externally forced or perturbed. The system matrix  $A$  is also referred to as the *adjacency matrix* following a graph theoretic view on the dynamics. The key novelty in our work is in considering *sparse* systems, i.e., sparse matrices  $A$ .

**Discussion of assumptions and limitations.** Linearity, autonomy, homogeneity and the absence of noise heavily restrict the types of systems studied in our work. The linearity assumption is in line with existing work [Stanhope et al., 2014, Qiu et al., 2022, Fedoryuk, 2012, Ovchinnikov et al., 2022] and required for the feasibility of theoretical analysis. Autonomy and homogeneity are adopted to represent our focus on passive observations of naturally evolving systems without external forcing, which corresponds closely to the idea of an observational distribution in the causal inference literature and differentiates our work from approaches towards controllability/observability in the (optimal) control and system identification literature. Some of the existing work on identifying linear ODEs from a single trajectory have been extended to post-nonlinear models (breaking linearity) [Miao et al., 2011], affine systems (extending homogeneity) [Duan et al., 2020], and include discrete, noisy observations [Wang et al., 2024]. We believe these works offer fruitful pointers towards extending our analysis of sparse systems here beyond its current limitations. At the same time, Scholl et al. [2023] show that in more general non-linear function classes identifiability requires observing trajectories that essentially “cover the entire state space”, putting theoretical limits on what one can hope for in generic non-linear settings. More implicitly, we also assume full observations, i.e., that the entire state relevant for the evolution of the system can be observed. In many practical settings, one may be limited by partial observability. Existing results indicate that identifiability is generally impossible in such settings without strong assumptions on the observation function [Cobelli and Romanin-Jacur, 2007], which is why partial observations are beyond the scope of this work.

**Main goal.** Our main goal is to answer the following question: Given a trajectory  $x : [0, T] \rightarrow \mathbb{R}^n$  that solves the IVP in Eq. (1), (when) can we uniquely infer  $A$  under the assumption that  $A$  is sparse?

Let us first formalize and concretize this identifiability problem.

**Definition 1** (identifiability from  $x$  in  $\Omega \subseteq \mathbb{R}^{n \times n}$ ). *Let  $A \in \Omega \subseteq \mathbb{R}^{n \times n}$  and let  $x : [0, T] \rightarrow \mathbb{R}^n$  be a solution of  $\dot{x}(t) := \frac{dx}{dt}(t) = Ax(t)$ . We call  $A$  **identifiable from  $x$  in  $\Omega$**  if there exists no  $B \in \Omega$  with  $\frac{dx}{dt}(t) = Bx(t)$ .*

**Remarks.** The IVP in Eq. (1) has a unique solution  $x$  on all of  $\mathbb{R}$  for all  $A$  and  $x_0$  by the Picard-Lindelöf theorem and the fact that linear functions are globally Lipschitz [Arnold, 1992]. Therefore, instead of  $[0, T]$  we can use any interval (including all of  $\mathbb{R}$ ) as time interval in Definition 1. In this work, we are specifically interested in identifying  $A$  for a given observed trajectory. Related but different notions of identifiability studied in the literature include, for example [Stanhope et al., 2014, Qiu et al., 2022]: (a) For a fixed initial condition  $x_0 \in \mathbb{R}^n$ , all pairs of distinct systems  $A, B \in \Omega$  lead to different trajectories. (b) For all pairs of distinct systems  $A, B \in \Omega$ , there exists some initial condition  $x_0 \in \mathbb{R}^n$  leading to different trajectories. (c) For all pairs of distinct systems  $A, B \in \Omega$ , every initial condition  $x_0 \in \mathbb{R}^n$  leads to distinct trajectories. It is easy to see that notion (b) is true “globally,” i.e., even for  $\Omega = \mathbb{R}^{n \times n}$  [Stanhope et al., 2014]. This relates closely to the typical linear time invariant (LTI) setting in system identification including controls: when we can “probe” the system by choosing different initial conditions as controls, we are always able to identify it fully. Instead, we concretely focus on identifiability from merely observational data in the form of a single solution trajectory. On the flip side, (c) is not true for  $\Omega = \mathbb{R}^{n \times n}$  (and does not even hold for “most”  $\Omega \subseteq \mathbb{R}^{n \times n}$ , see Qiu et al., 2022, Sec. S1). This is primarily due to the existence of “unlucky” initial conditions, which we will make rigorous below.

To decide when a system can be identified from a given trajectory, it is useful to characterize whether there are systems for which this is never possible. Throughout this work, we will primarily focus on the setting where  $\Omega = \mathbb{R}^{n \times n}$  reflecting the fact that we typically cannot exclude any systems from potentially being the ground truth, while still allowing for different probability measures on  $\Omega$ .

**Definition 2** (global unidentifiability). *We call  $A \in \mathbb{R}^{n \times n}$  **globally unidentifiable** in  $\Omega$ , if there exists no  $x_0 \in \mathbb{R}^n$  such that  $A$  is identifiable from the corresponding solution trajectory  $x$  in  $\mathbb{R}^{n \times n}$ . We denote the set of all globally unidentifiable  $A$  by  $\mathcal{U} \subseteq \mathbb{R}^{n \times n}$ .*

In words, a system  $A$  is globally unidentifiable if any solution trajectory is also the solution to some other system  $B$  (this need not be a single alternative  $B$ , but for each trajectory there must exist at least one). A necessary and sufficient condition for global unidentifiability that characterizes these “hopeless” systems reads as follows.

**Theorem 1** (Stanhope et al., 2014, Thm 2.5 + Thm 3.6). *A system  $A \in \mathbb{R}^{n \times n}$  is globally unidentifiable if and only if it has more than one Jordan block corresponding to the same eigenvalue (for at least one eigenvalue) in the Jordan normal form of  $A$ .*

Additionally, they also characterized when  $A$  is identifiable from  $x$ .

**Theorem 2** (Stanhope et al., 2014, Lem 3.4 + Thm 3.4). *A system  $A \in \mathbb{R}^{n \times n}$  is identifiable from  $x$  if and only if  $x(0)$  is not contained in any  $A$ -invariant proper subspace of  $\mathbb{R}^n$ .*

Whenever any point along the solution trajectory (e.g., the initial condition) lies in an  $A$ -invariant proper subspace of  $A$ , the entire trajectory will be confined to this subspace. The trajectory is thus not “probing” the complement of this linear subspace in  $\mathbb{R}^{n \times n}$ . Thus we can construct another system  $B$  that agrees with  $A$  (viewed as linear maps) on the  $A$ -invariant subspace, but differs from  $A$  on the complement.

### 3 Global unidentifiability

We will refer to  $A$  being in  $\mathcal{U}$  as “system level unidentifiability,” because when  $A \in \mathcal{U}$  it is unidentifiable regardless of the observed trajectory. For all  $A \notin \mathcal{U}$ , there exists at least one solution trajectory  $x$ , such that  $A$  is identifiable from  $x$  in  $\mathbb{R}^{n \times n}$ . However, there may still be “unlucky”  $x$ , namely those confined to an  $A$ -invariant proper subspace, for which  $A$  remains unidentifiable. For any system  $A$ , we define  $\mathcal{U}_A \subseteq \mathbb{R}^n$  to be the set of initial conditions  $x_0 \in \mathbb{R}^n$  from which  $A$  is not identifiable. We call this “trajectory level unidentifiability”.

Ultimately, our main goal aims at quantifying whether we should expect to be able to identify “a random system” from “a random solution trajectory.” To formalize this question, consider a joint probability distribution  $P_{A, \mathbf{x}_0}$  over pairs of systems and initial conditions  $(A, \mathbf{x}_0) \in \mathbb{R}^{n \times n} \times \mathbb{R}^n$  (equipped with the Borel- $\sigma$ -algebra). We are then interested in

$$\begin{aligned} P_{A, \mathbf{x}_0}(A \text{ not identifiable from } \mathbf{x}_0) &= \int P_{A, \mathbf{x}_0}(\mathcal{U}_A \mid A) dP_A(A) \\ &= P_A(\mathcal{U}) + \int \chi_{A \notin \mathcal{U}_A}(A) P_{A, \mathbf{x}_0}(\mathcal{U}_A \mid A) dP_A(A), \end{aligned} \quad (2)$$

where  $\chi$  is the indicator function, i.e.,  $\chi_{A \notin \mathcal{U}_A}(A) = 1$  if  $A \notin \mathcal{U}$  and 0 otherwise. The partitioning in the last equality corresponds to a two-step reasoning: What is the probability of hitting a globally unidentifiable system (on the system identification level) and, separately, for any non globally unidentifiable model, what is the probability of hitting an “unlucky” initial condition.<sup>1</sup>

Before developing a lower bound for Eq. (2), we introduce the assumed sparsity model.

**Definition 3** (Sparse-Continuous Ensemble). *We call a matrix  $A := (B_{ij}X_{ij})_{i,j=1}^n$  with  $B_{ij} \sim \text{Ber}(1-p)$  independent Bernoulli random variables for some  $p \in [0, 1]$ , and  $X_{ij} \sim P_X$  independent continuous random variables (i.e., their distribution is absolutely continuous with respect to the Lebesgue measure on  $\mathbb{R}$ ), a **sparse-continuous** random matrix (or system) with sparsity level  $p$ .*

Examples include any iid sub-Gaussian random matrix masked by iid Bernoulli variables.

**Lemma 1.** *For a sparse-continuous random matrix  $A$ , the probability that  $A$  has repeated nonzero eigenvalues is zero. In other words,*

$$P_A(\{A \in \mathbb{R}^{n \times n} \mid \exists \lambda \in \mathbb{R} : \text{rank}(A - \lambda I) < n - 1\}) = P_A(\{A \in \mathbb{R}^{n \times n} \mid \text{rank}(A) < n - 1\}).$$

*Proof.* For a fixed zero-pattern  $S \subseteq [n]^2$  (specifying which entries are nonzero) define

$$E_S := \{\omega \mid B_{ij}(\omega) = 1 \text{ if and only if } (i, j) \in S\} \cap \{\omega \mid A(\omega) \text{ has a repeated nonzero eigenvalue}\}.$$

We have  $P(\{S(\omega) = S\}) = p^{|S|}(1-p)^{n^2-|S|}$  and conditionally on  $S(\omega) = S$ ,  $A(\omega)$  is a vector of  $|S|$  continuous random variables  $(X_{ij})_{(i,j) \in S}$  that is absolutely continuous with respect to the Lebesgue measure on  $\mathbb{R}^{|S|}$ . The matrix  $A$  has a repeated nonzero eigenvalue if there exists an eigenvalue  $\lambda \neq 0$  of algebraic multiplicity at least 2, i.e.,  $\det(A - \lambda I) = 0$  and  $\frac{d}{d\lambda} \det(A - \lambda I) = 0$ . These conditions define a nontrivial algebraic subset in  $\mathbb{R}^{n \times n}$ , imposing polynomial equations on these  $|S|$  nonzero entries. These polynomials vanish only on a measure-zero subset of  $\mathbb{R}^{|S|}$  (since the polynomials are not identically zero). Thus,  $P(E_S) = 0$ . And by the union bound,

$$P(\{A \text{ has a repeated nonzero eigenvalue}\}) \leq \sum_{S \subseteq [n]^2} P(E_S) = 0.$$

The second statement follows since the two events characterize having *some* repeated eigenvalue and *zero* being a repeated eigenvalue, respectively.  $\square$

With these preliminaries, we find the following lower bound.

**Lemma 2.** *A sparse-continuous random matrix with sparsity  $p$  is globally not identifiable with probability at least  $1 - (1 - p^n)^n - np^n(1 - p^n)^{n-1}$  for  $n \geq 2$  (and  $p$  for  $n = 1$ ).*

The proof of this lemma can be found in Appendix A. This bound is driven by the presence of zero rows/columns. These correspond to sink or source nodes in the corresponding adjacency graph, which are typically frequent in sparse graphs and dominate the probability of rank deficiency compared to events that require repeated rows/columns with identical zero patterns that are not all zero. We also provide a sharp threshold on the dimension  $n$  and sparsity level  $p$  for global unidentifiability in the following lemma.

<sup>1</sup>The negation of “globally unidentifiable” is not called “globally identifiable” as this would convey the wrong impression of it being “always” identifiable, i.e., from any initial condition.

**Lemma 3** (sharp threshold for global unidentifiability). *Let  $A$  be a sparse-continuous matrix with  $n$ -dependent sparsity level  $p(n)$ . Then, for  $p_c(n) = 1 - \frac{\ln(n)}{n}$  and any function  $\omega(n) \rightarrow \infty$  we have the if  $p(n) = p_c(n) + \frac{\omega(n)}{n}$ , then  $P(\text{rank}(A) \leq n-2) \rightarrow 1$  for  $n \rightarrow \infty$  and if  $p(n) = p_c(n) - \frac{\omega(n)}{n}$ , then  $P(\text{rank}(A) \leq n-2) \rightarrow 0$  for  $n \rightarrow \infty$ . That is, there is a threshold at  $p = \ln(n)/n$  decisive for whether  $A$  is asymptotically globally unidentifiable with high probability or not.*

The proof can be found in Appendix A. This is consistent with known results on Bernoulli matrices (e.g., Frieze and Karoński, 2015, Basak and Rudelson, 2021) where there exists a similar sharp transition at  $p = 1 - \ln(n)/n$  for the probability of singularity. Our proof extends the same threshold to two-fold rank deficiency in sparse-continuous matrices and thus to global unidentifiability.

In practice, numerically evaluating matrix ranks requires thresholding. By the Eckart–Young–Mirsky theorem the second smallest singular value of  $\sigma_2$  of  $A$  corresponds to the distance of  $A$  the closest matrix  $A'$  with  $\text{rank}(A') < n-1$ . As such it provides a robust continuous numerical measure of system unidentifiability.

## 4 Trajectory unidentifiability

We now turn to “trajectory unidentifiability”, i.e., the situation where  $A$  is not globally unidentifiable, yet it may be unidentifiable from specific observed trajectories  $\mathbf{x}$ . Let  $(A, \mathbf{x}_0) \sim P_A \otimes P_{\mathbf{x}_0}$  with an absolutely continuous  $P_{\mathbf{x}_0}$  (w.r.t. the Lebesgue measure on  $\mathbb{R}^n$ ) and  $P_A$  the distribution of a sparse-continuous matrix  $A$ . Since, according to Theorem 2,  $A$  is unidentifiable from  $\mathbf{x}$  if and only if  $\mathbf{x}_0$  is in a proper invariant subspace of  $A$ , and the fact that any *proper* subspace of  $\mathbb{R}^n$  has zero probability under any absolutely continuous probability measure (with respect to the Lebesgue measure), we conclude that  $P_{A, \mathbf{x}_0}(\mathcal{U}_A \mid A = A') = 0$  for all  $A' \notin \mathcal{U}$ . Therefore, the second term in Eq. (2) is zero. The probability of a “random”  $A$  being identifiable from a “random” solution trajectory is thus given entirely by the probability of  $A$  being globally unidentifiable—the probability of “unlucky” initial conditions is zero.

However,  $\mathbf{x}_0$  being close to a proper  $A$ -invariant subspace can still be problematic in practice, which we later demonstrate empirically. To measure this “closeness to unidentifiability”, we define

$$d_A : \mathbb{R}^n \rightarrow [0, 1], \quad \mathbf{x}_0 \mapsto \frac{1}{\|\mathbf{x}_0\|_2} \min\{\text{dist}(\mathbf{x}_0, V) \mid V \in \mathcal{I}(A)\}, \quad (3)$$

where  $\mathcal{I}(A)$  is the set of proper  $A$ -invariant linear subspaces of  $\mathbb{R}^n$  and  $\text{dist}(\mathbf{x}_0, V) := \min_{\mathbf{y} \in V} \|\mathbf{x}_0 - \mathbf{y}\|_2$  is the Euclidean distance of  $\mathbf{x}_0$  from the subspace  $V$ . We have that  $d_A(\mathbf{x}_0) = 0$  if and only if  $\mathbf{x}_0$  lies in a proper  $A$ -invariant subspace, and  $d_A$  provides a continuous measure for the “level of unidentifiability from the trajectory,” formalized as follows.

**Lemma 4.** *Let  $A, A' \in \mathbb{R}^{n \times n}$  and assume there is an  $A$ -invariant subspace  $V^*$  such that  $(A - A')V^* = \{0\}$ . Then, for every  $t \geq 0$  and  $\mathbf{x}_0 \in \mathbb{R}^n$ , we have that*

$$\|e^{At}\mathbf{x}_0 - e^{A't}\mathbf{x}_0\|_2 \leq C(t, A, A')\|A - A'\|_2 d_A(\mathbf{x}_0)$$

with  $C(t, A, A') := \int_0^t \|e^{A(t-s)}\|_2 \|e^{A's}\|_2 ds$ . Further, for any  $\varepsilon > 0$ , the condition

$$\|(e^{At} - e^{A't})\mathbf{x}_0\| \leq \varepsilon \quad \text{for all } 0 \leq t \leq T$$

holds whenever

$$T \leq \frac{1}{\alpha} W\left(\alpha \frac{\varepsilon}{\|A - A'\| M^2 d_A(\mathbf{x}_0)}\right),$$

where  $W(\cdot)$  denotes the Lambert function and constants  $\alpha \in \mathbb{R}$ ,  $M \geq 1$  such that  $\|e^{At}\|, \|e^{A't}\| \leq Me^{\alpha t}$  for all  $t \geq 0$ .

The proof can be found in Appendix A. Assume  $A$  is identifiable from  $\mathbf{x}_0$ , but  $\mathbf{x}_0$  is close to a proper  $A$ -invariant subspace  $V^*$  with distance  $d_A(\mathbf{x}_0)$ . Then there exists another  $A' \neq A$  that agrees with  $A$  on  $V^*$ , i.e.,  $A'$  could practically be mistaken for the underlying true dynamic. Lemma 4 states that the trajectories under such  $A$  and  $A'$  indeed stay  $\varepsilon$ -close to each other up until time  $T$ .



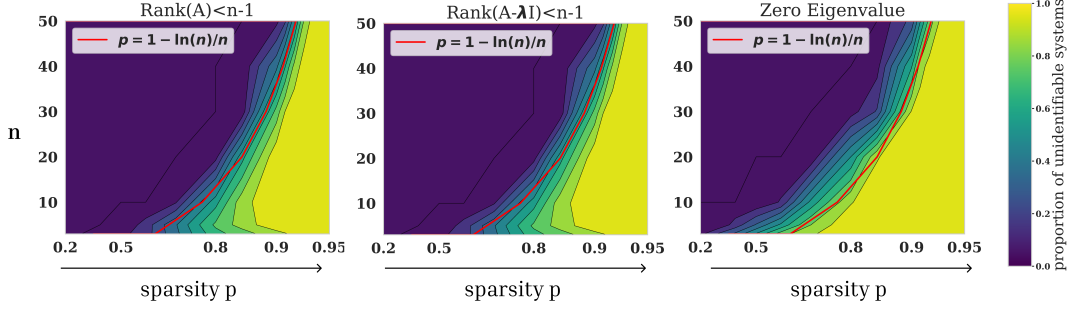


Figure 2: Proportion of matrices satisfying the conditions i), ii) and iii) at different system dimensions  $n$  and sparsity levels  $p$ . All three conditions exhibit a sharp increase in frequency with higher sparsity, consistent with the threshold  $p = 1 - \ln(n)/n$ .

## 5 Empirical results

Our empirical validation experiments include three distinct viewpoints: firstly, we assume the true system matrix to be available in order to confirm our theoretical results on unidentifiability in sparse matrices in principle. Secondly, we assume that we only have observed trajectories at hand and evaluate trajectory-level identifiability criteria. While these results assess whether a system is (or is not) identifiable, we finally also empirically assess the performance of two widely used estimators that attempt to learn the underlying system from data directly, hence zooming in on identifiability challenges in practice.

**Data generation.** We focus on systems of dimensions  $n \in \mathcal{D} := \{3, 5, 10, 20, 30, 40, 50\}$  and sparsity levels  $p \in \mathcal{P} = \{0.1, 0.2, 0.3, 0.4, 0.5, 0.6, 0.7, 0.8, 0.9, 0.95, 1.0\}$ .<sup>2</sup> For each  $(n, p) \in \mathcal{D} \times \mathcal{P}$ , we generate 100 matrices according to the sparse-continuous model in Definition 3 and take a standard normal for the continuous distribution  $P_X = \mathcal{N}(0, 1)$ . For each matrix, we sample 100 initial conditions uniformly from the unit circle in  $\mathbb{R}^n$  and solve the corresponding trajectories numerically over the interval  $t \in [0, 1]$  using a standard explicit RK45 solver with 512 homogeneous time steps. Results for different random matrix models, for example disallowing zero rows/columns, can be found in Appendix B.

### 5.1 System-level unidentifiability

In this section, we perform an exploratory analysis of global unidentifiability conditions by examining properties at the system level. The contour map in Fig. 2 illustrates, for varying values of sparsity  $p$  and dimension  $n$ , the empirical frequency with which the generated system matrices  $A$  violate at least one of three structural criteria: (i)  $\text{rank}(A) < n - 1$ ; (ii) there exists an eigenvalue  $\lambda$  for which  $\text{rank}(A - \lambda I) < n - 1$ ; or (iii) the spectrum contains the zero eigenvalue. As matrices become sparser (i.e., as  $p$  increases), the proportion of globally unidentifiable matrices sharply increases. Notably, the nearly identical contour plots for conditions (i) and (ii) strongly support our theoretical result stated in Lemma 1. Moreover, the condition regarding the existence of zero eigenvalues aligns closely with the theoretical threshold  $p = 1 - \frac{\ln(n)}{n}$  (depicted by the red curve).

**Discussion on realistic sparsity levels.** Although global (system-level) unidentifiability becomes less critical as the dimension increases (consistent with the threshold  $p = 1 - \frac{\ln(n)}{n}$ ), seemingly only leaving systems of negligibly high sparsity-levels unidentifiable, we emphasize that such high sparsity regimes are not merely theoretical but are indeed realistic and frequently encountered in real-world scenarios. For instance, the *P. trichocarpa* PEN gold standard network [Walker et al., 2022], introduced earlier, has a sparsity level of approximately 0.997 for a graph comprising 1690 nodes (genes), exceeding the theoretical threshold  $p^* = 1 - \frac{\ln(n)}{n} \approx 0.996$ . Similarly, the *E. coli* gene regulatory network [Walker et al., 2022], consisting of 1222 genes, exhibits a sparsity of about 0.999, surpassing its corresponding threshold of  $p^* = 0.995$ .

<sup>2</sup>Recall that higher  $p$  for us corresponds to “more zeros.”

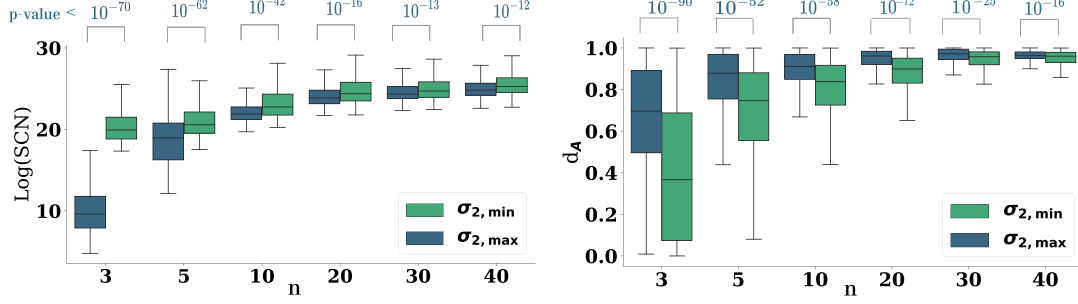


Figure 3: Box-plots of smoothed condition numbers (SCN) and distance-to-unidentifiability  $d_A$  for the least and most identifiable groups of systems at different dimensions  $n$ .

## 5.2 Trajectory-level unidentifiability

Following the argument in Section 3, the second-smallest singular value  $\sigma_2$  of a system relates to its global unidentifiability. Here, we ask whether systems with worse global unidentifiability metrics also give rise to trajectories that are statistically less identifiable. To address this question, we rank the generated system matrices by their second-smallest singular value  $\sigma_2$  for each combination of dimension  $n$  and sparsity  $p$ . Matrices with  $\sigma_2$  falling into the top-10% of ranked singular values are subsequently referred to as  $A_{\sigma_2, \max}$ , similarly matrices at the bottom-10% are referred to as  $A_{\sigma_2, \min}$ .

To determine whether the trajectories produced by these two matrix groups differ in identifiability, we compared the sample means of two complementary trajectory-level identifiability metrics: our closeness-to-unidentifiability distance  $d_{A,0}(x_0)$  from Section 4 (larger implies more likely identifiable) as well as the smoothed condition number (SCN) as established by Qiu et al. [2022] (smaller implies more likely identifiable). Specifically, we approximate  $d_A(x_0)$  by the normalized distance of the initial state to  $\ker(A)$ , using the metric

$$d_A(x_0) \approx d_{A,0}(x_0) := \frac{1}{\|x_0\|} \text{dist}(x_0, \ker(A)) \in [0, 1]. \quad (4)$$

Compared to  $d_A(x_0)$ ,  $d_{A,0}(x_0)$  allows us to estimate “distance-to-unidentifiability” without analyzing all proper  $A$ -invariant subspaces. As a second criterion, we evaluate the invertibility of the pairwise inner product matrix, as established by Qiu et al. [2022], who showed that a trajectory  $x(t \mid A, x_0)$  is identifiable if and only if the pairwise inner product matrix  $\Sigma_{xx} = \langle x(t), x(t) \rangle_{i,j} = \int_0^T x_i(t)x_j(t)dt$  is invertible. Qiu et al. [2022] offer a straightforward method for approximating  $\Sigma_{xx}$ , and introduce the Smoothed Condition Number (SCN)  $k(\Sigma_{xx})$  as the condition number of  $\Sigma_{xx}$ .

**Results.** Boxplots of SCN and  $d_A$  values are depicted in Fig. 3 at different dimensions  $n$ . For each  $n$  we focus on the sparsity parameter  $p^*$  closest to the threshold  $1 - \ln(n)/n$ , which corresponds to the critical sparsity value at which a system becomes unidentifiable. We use Welch’s t-test with one-sided alternatives that reflect the expected direction of the difference:

$$\begin{aligned} \text{SCN:} \quad & H_0 : \mu_{A_{\sigma_2, \max}}^{\text{SCN}} \geq \mu_{A_{\sigma_2, \min}}^{\text{SCN}} & H_1 : \mu_{A_{\sigma_2, \max}}^{\text{SCN}} < \mu_{A_{\sigma_2, \min}}^{\text{SCN}} \\ d_{A,0}(x_0) : \quad & H_0 : \mu_{A_{\sigma_2, \min}}^{d_A} \geq \mu_{A_{\sigma_2, \max}}^{d_A} & H_1 : \mu_{A_{\sigma_2, \min}}^{d_A} < \mu_{A_{\sigma_2, \max}}^{d_A} \end{aligned}$$

Here  $\mu_{A_{\sigma_2, \max}}$  and  $\mu_{A_{\sigma_2, \min}}$  denote the population means in the two subgroups. The goal of the statistical test is to establish whether the two subgroups truly differ in trajectory-identifiability performance. We find that systems or subgroup  $A_{\sigma_2, \min}$  are significantly less probable to identify ( $p \ll 0.01$ ) for all system dimensions and both criteria. These results are consistent with our theoretical derivations and also in line with the previously analyzed systems-level criteria

## 5.3 Empirical Unidentifiability

We evaluate the performance of two state-of-the-art models for identifying dynamical systems: Neural ODEs (**NODEs**) [Chen et al., 2018], which approximate dynamics through a neural-network-based function  $f_\theta(x(t))$ , as well as the Sparse Identification of Nonlinear Dynamics algorithm (**SINDy**)



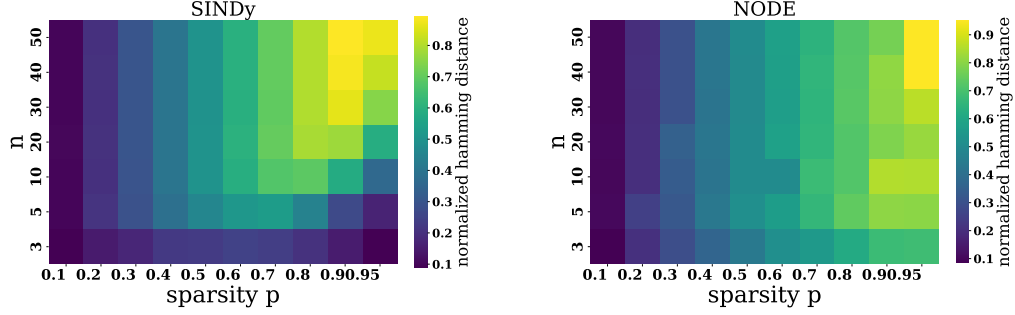


Figure 4: Normalized Hamming distance of reconstructed systems using SINDy (left) and NODE (right) across varying dimensions and sparsity levels. Reconstruction accuracy declines noticeably with increasing dimensionality and sparsity.

[Brunton et al., 2016], which employs  $L_2$ -regularized linear regression on a predefined set of basis functions. To effectively model sparse linear systems, we utilize an  $L_1$ -regularized neural network without activation functions for NODEs, and linear basis functions for SINDy. Hyper-parameters for both models are tuned per system. More details on the methods can be found in Appendix B.3.

Since we are less interested in the question of whether the model can fit the observed data overall, but rather in the question of whether the models correctly identify the underlying system matrices  $A$  in cases where they do fit the data well, we filter out estimates for which the corresponding reconstruction of the observed trajectory does not satisfy prescribed  $R^2$  and MSE thresholds, where these metrics compare observed and reconstructed trajectories. This best-case filtering ensures that subsequent empirical results can be tied to identifiability properties rather than potential issues with model optimization or architecture.

**Results.** As perfect point estimates of all coefficients of system matrix  $A$  are unreasonable to expect (e.g. due to numerical issues), we instead use the Hamming distance to compare binarized ground truth  $A$  and estimate  $\hat{A}$ , which we additionally normalize by  $n$  for comparability across dimensions. The Hamming distance corresponds to the number of matching symbols (here: zero or one) and thus captures the overlap of the predicted and true sparsity patterns. The heatmaps in Fig. 4 show for both SINDy and NODE a clear left-right gradient, indicating that sparse systems lead to a larger Hamming distances - consistent with our theoretical finding that higher sparsity increases the probability of unidentifiability. Exemplary model estimates and corresponding trajectory fits are displayed for a selected dense and sparse system in Fig. 1 which further illustrate the phenomenon.

## 6 Conclusion

In this work, we focus on identifiability of sparse linear ODEs  $A$  from a single observed trajectory  $\mathbf{x}$ . We first partition the probability of unidentifiability of  $A$  from  $\mathbf{x}$  into “system level unidentifiability” ( $A \in \mathcal{U}$ ) and “trajectory level unidentifiability”, i.e., hitting an “unlucky” initial condition. After showing that the latter scenario almost surely does not happen, we show that in sparse systems the probability of unidentifiability can be lower bounded by a positive quantity and exhibits a sharp asymptotic threshold at  $p = 1 - \ln(n)/n$  for global unidentifiability. This puts an important asterisk on the celebrated result that “almost all linear ODEs are identifiable,” which ceases to hold under sparsity, which is often a core underlying assumption in dynamical system modeling. We go on to empirically verify that theoretical unidentifiability is a serious practical challenge and extend our analysis to near-unidentifiability on the “trajectory level,” demonstrating that the theoretically negligible case of unlucky initial conditions further exacerbates the problem. Important directions for future work include extending our results to affine and post-nonlinear models, noisy or partially observed systems, multiple observed trajectories, and deriving computable metrics for practical unidentifiability from data alone.

## Acknowledgments and disclosure of funding

This work is supported by the DAAD programme Konrad Zuse Schools of Excellence in Artificial Intelligence, sponsored by the Federal Ministry of Education and Research. This work has been supported by the German Federal Ministry of Education and Research (Grant: 01IS24082). The authors gratefully acknowledge the Gauss Centre for Supercomputing e.V. ([www.gauss-centre.eu](http://www.gauss-centre.eu)) for funding this project by providing computing time through the John von Neumann Institute for Computing (NIC) on the GCS Supercomputer JUWELS at Jülich Supercomputing Centre (JSC).

## References

- Hananeh Aliee, Fabian J Theis, and Niki Kilbertus. Beyond predictions in neural odes: Identification and interventions. *arXiv preprint arXiv:2106.12430*, 2021.
- Hananeh Aliee, Till Richter, Mikhail Solonin, Ignacio Ibarra, Fabian Theis, and Niki Kilbertus. Sparsity in continuous-depth neural networks. *Advances in Neural Information Processing Systems*, 35:901–914, 2022.
- Vladimir I Arnold. *Ordinary differential equations*. Springer Science & Business Media, 1992.
- Brian Bartoldson, Ari Morcos, Adrian Barbu, and Gordon Erlebacher. The generalization-stability tradeoff in neural network pruning. *Advances in Neural Information Processing Systems*, 33: 20852–20864, 2020.
- Anirban Basak and Mark Rudelson. Sharp transition of the invertibility of the adjacency matrices of sparse random graphs. *Probability theory and related fields*, 180:233–308, 2021.
- Sören Becker, Michal Klein, Alexander Neitz, Giambattista Parascandolo, and Niki Kilbertus. Predicting ordinary differential equations with transformers. In *International conference on machine learning*, pages 1978–2002. PMLR, 2023.
- Ror Bellman and Karl Johan Åström. On structural identifiability. *Mathematical biosciences*, 7(3-4): 329–339, 1970.
- Alexis Bellot, Kim Branson, and Mihaela van der Schaar. Neural graphical modelling in continuous-time: consistency guarantees and algorithms. *arXiv preprint arXiv:2105.02522*, 2021.
- James Bradbury, Roy Frostig, Peter Hawkins, Matthew James Johnson, Chris Leary, Dougal Maclaurin, George Necula, Adam Paszke, Jake VanderPlas, Skye Wanderman-Milne, and Qiao Zhang. JAX: composable transformations of Python+NumPy programs, 2018. URL <http://github.com/google/jax>.
- Steven L. Brunton, Joshua L. Proctor, and J. Nathan Kutz. Discovering governing equations from data by sparse identification of nonlinear dynamical systems. *Proceedings of the National Academy of Sciences*, 113(15):3932–3937, 2016. ISSN 0027-8424. doi: 10.1073/pnas.1517384113. URL <https://www.pnas.org/content/113/15/3932>.
- Michelle Carey, Juan Camilo Ramírez, Shuang Wu, and Hulin Wu. A big data pipeline: Identifying dynamic gene regulatory networks from time-course gene expression omnibus data with applications to influenza infection. *Statistical methods in medical research*, 27(7):1930–1955, 2018.
- Ricky TQ Chen, Yulia Rubanova, Jesse Bettencourt, and David K Duvenaud. Neural ordinary differential equations. *Advances in neural information processing systems*, 31, 2018.
- Claudio Cobelli and Giorgio Romanin-Jacur. Controllability, observability and structural identifiability of multi input and multi output biological compartmental systems. *IEEE Transactions on Biomedical Engineering*, 2007.
- Daniel Commenges, D Jolly, Julia Drylewicz, Hein Putter, and Rodolphe Thiébaud. Inference in hiv dynamics models via hierarchical likelihood. *Computational Statistics & Data Analysis*, 55(1): 446–456, 2011.

- Nik Cunniffe, Frédéric Hamelin, Abderrahman Iggidr, Alain Rapaport, and Gauthier Sallet. *Identifiability and Observability in Epidemiological Models*. Springer, 2024.
- Stéphane d’Ascoli, Sören Becker, Alexander Mathis, Philippe Schwaller, and Niki Kilbertus. Odeformer: Symbolic regression of dynamical systems with transformers. In *International Conference on Learning Representations*, 2024.
- Brian de Silva, Kathleen Champion, Markus Quade, Jean-Christophe Loiseau, J Nathan Kutz, and Steven Brunton. PySINDy: A Python package for the sparse identification of nonlinear dynamical systems from data. *Journal of Open Source Software*, 5(49):1–4, 2020.
- Yi Ding and Panos Toulis. Dynamical systems theory for causal inference with application to synthetic control methods. In *International Conference on Artificial Intelligence and Statistics*, pages 1888–1898. PMLR, 2020.
- Jérémy Donà, Marie Déchelle, Marina Levy, and Patrick Gallinari. Constrained physical-statistics models for dynamical system identification and prediction. In *ICLR 2022-The Tenth International Conference on Learning Representations*, 2022.
- X Duan, JE Rubin, and D Swigon. Identification of affine dynamical systems from a single trajectory. *Inverse Problems*, 36(8):085004, 2020.
- Mikhail V Fedoryuk. *Asymptotic analysis: linear ordinary differential equations*. Springer Science & Business Media, 2012.
- Alan Frieze and Michał Karoński. *Introduction to random graphs*. Cambridge University Press, 2015.
- BC Gargash and DP Mital. A necessary and sufficient condition of global structural identifiability of compartmental models. *Computers in biology and medicine*, 10(4):237–242, 1980.
- Eric A. Hagberg, Daniel A. Schult, and Pieter J. Swart. Exploring network structure, dynamics, and function using networkx. In Gaël Varoquaux, Travis Vaught, and Jarrod Millman, editors, *Proceedings of the 7th Python in Science Conference*, pages 11 – 15, Pasadena, CA USA, 2008.
- Charles R Harris, K Jarrod Millman, Stéfan J van der Walt, Ralf Gommers, Pauli Virtanen, David Cournapeau, Eric Wieser, Julian Taylor, Sebastian Berg, Nathaniel J Smith, Robert Kern, Matti Picus, Stephan Hoyer, Marten H van Kerkwijk, Matthew Brett, Allan Haldane, Jaime Fernández del Río, Mark Wiebe, Pearu Peterson, Pierre Gérard-Marchant, Kevin Sheppard, Tyler Reddy, Warren Weckesser, Hameer Abbasi, Christoph Gohlke, and Travis E Oliphant. Array programming with NumPy. *Nature*, 2020.
- Yangxin Huang, Dacheng Liu, and Hulin Wu. Hierarchical bayesian methods for estimation of parameters in a longitudinal hiv dynamic system. *Biometrics*, 62(2):413–423, 2006.
- John D Hunter. Matplotlib: A 2D graphics environment. *Computing in Science & Engineering*, 2007.
- Marc Lavielle, Adeline Samson, Ana Karina Fermin, and France Mentré. Maximum likelihood estimation of long-term hiv dynamic models and antiviral response. *Biometrics*, 67(1):250–259, 2011.
- Zhengfeng Li, Michael R Osborne, and Tania Prvan. Parameter estimation of ordinary differential equations. *IMA Journal of Numerical Analysis*, 25(2):264–285, 2005.
- David Liben-Nowell. *An algorithmic approach to social networks*. PhD thesis, Massachusetts Institute of Technology, 2005.
- Marten Lienen and Stephan Günnemann. torchode: A parallel ODE solver for pytorch. In *The Symbiosis of Deep Learning and Differential Equations II, NeurIPS*, 2022. URL <https://openreview.net/forum?id=uiKVKTiUYB0>.
- Tao Lu, Hua Liang, Hongzhe Li, and Hulin Wu. High-dimensional odes coupled with mixed-effects modeling techniques for dynamic gene regulatory network identification. *Journal of the American Statistical Association*, 106(496):1242–1258, 2011.

- Hongyu Miao, Xiaohua Xia, Alan S Perelson, and Hulin Wu. On identifiability of nonlinear ode models and applications in viral dynamics. *SIAM review*, 53(1):3–39, 2011.
- R Muñoz-Tamayo, L Puillet, JB Daniel, D Sauvant, O Martin, M Taghipoor, and P Blavy. Review: To be or not to be an identifiable model. is this a relevant question in animal science modelling? *animal*, 12, 701–712, 2018.
- Alexey Ovchinnikov, Gleb Pogudin, and Peter Thompson. Input-output equations and identifiability of linear ode models. *IEEE Transactions on Automatic Control*, 68(2):812–824, 2022.
- The pandas development team. pandas-dev/pandas: Pandas, February 2020. URL <https://doi.org/10.5281/zenodo.3509134>.
- Adam Paszke, Sam Gross, Francisco Massa, Adam Lerer, James Bradbury, Gregory Chanan, Trevor Killeen, Zeming Lin, Natalia Gimelshein, Luca Antiga, Alban Desmaison, Andreas Kopf, Edward Yang, Zachary DeVito, Martin Raison, Alykhan Tejani, Sasank Chilamkurthy, Benoit Steiner, Lu Fang, Junjie Bai, and Soumith Chintala. PyTorch: An imperative style, high-performance deep learning library. In *NeurIPS*, 2019.
- Fabian Pedregosa, Gaël Varoquaux, Alexandre Gramfort, Vincent Michel, Bertrand Thirion, Olivier Grisel, Mathieu Blondel, Peter Prettenhofer, Ron Weiss, Vincent Dubourg, Jak Vanderplas, Alexandre Passos, David Cournapeau, Matthieu Brucher, Matthieu Perrot, and Édouard Duchesnay. Scikit-learn: Machine learning in Python. *JMLR*, 2011.
- Tong Qin, Kailiang Wu, and Dongbin Xiu. Data driven governing equations approximation using deep neural networks. *Journal of Computational Physics*, 395:620–635, 2019.
- Xing Qiu, Tao Xu, Babak Soltanalizadeh, and Hulin Wu. Identifiability analysis of linear ordinary differential equation systems with a single trajectory. *Applied Mathematics and Computation*, 430: 127260, 2022.
- A Raue, V Becker, U Klingmüller, and J Timmer. Identifiability and observability analysis for experimental design in nonlinear dynamical models. *Chaos: An Interdisciplinary Journal of Nonlinear Science*, 20(4), 2010.
- Chiara Ravazzi, Roberto Tempo, and Fabrizio Dabbene. Learning influence structure in sparse social networks. *IEEE Transactions on Control of Network Systems*, 5(4):1976–1986, 2017.
- Yulia Rubanova, Ricky TQ Chen, and David K Duvenaud. Latent ordinary differential equations for irregularly-sampled time series. *Advances in neural information processing systems*, 32, 2019.
- Maria Pia Saccomani. An effective automatic procedure for testing parameter identifiability of hiv/aids models. *Bulletin of mathematical biology*, 73:1734–1753, 2011.
- Philipp Scholl, Aras Bacho, Holger Boche, and Gitta Kutyniok. Symbolic recovery of differential equations: The identifiability problem. *arXiv preprint arXiv:2210.08342*, 2022.
- Philipp Scholl, Aras Bacho, Holger Boche, and Gitta Kutyniok. The uniqueness problem of physical law learning. In *ICASSP 2023-2023 IEEE International Conference on Acoustics, Speech and Signal Processing (ICASSP)*, pages 1–5. IEEE, 2023.
- Shelby Stanhope, Jonathan E Rubin, and David Swigon. Identifiability of linear and linear-in-parameters dynamical systems from a single trajectory. *SIAM Journal on Applied Dynamical Systems*, 13(4):1792–1815, 2014.
- Necibe Tuncer, Hayriye Gulbudak, Vincent L Cannataro, and Maia Martcheva. Structural and practical identifiability issues of immuno-epidemiological vector–host models with application to rift valley fever. *Bulletin of mathematical biology*, 78:1796–1827, 2016.
- Guido van Rossum and Fred L Drake. *Python 3 Reference Manual*. CreateSpace, 2009.
- Roman Vershynin. *High-dimensional probability: An introduction with applications in data science*, volume 47. Cambridge university press, 2018.

- Pauli Virtanen, Ralf Gommers, Travis E Oliphant, Matt Haberland, Tyler Reddy, David Cournapeau, Evgeni Burovski, Pearu Peterson, Warren Weckesser, Jonathan Bright, Stéfan J van der Walt, Matthew Brett, Joshua Wilson, K Jarrod Millman, Nikolay Mayorov, Andrew R J Nelson, Eric Jones, Robert Kern, Eric Larson, C J Carey, İlhan Polat, Yu Feng, Eric W Moore, Jake VanderPlas, Denis Laxalde, Josef Perktold, Robert Cimrman, Ian Henriksen, E A Quintero, Charles R Harris, Anne M Archibald, Antônio H Ribeiro, Fabian Pedregosa, Paul van Mulbregt, and SciPy 1.0 Contributors. SciPy 1.0: Fundamental Algorithms for Scientific Computing in Python. *Nature Methods*, 2020.
- Angelica M Walker, Ashley Cliff, Jonathon Romero, Manesh B Shah, Piet Jones, Joao Gabriel Felipe Machado Gazolla, Daniel A Jacobson, and David Kainer. Evaluating the performance of random forest and iterative random forest based methods when applied to gene expression data. *Computational and Structural Biotechnology Journal*, 20:3372–3386, 2022.
- Benjie Wang, Joel Jennings, and Wenbo Gong. Neural structure learning with stochastic differential equations. *arXiv preprint arXiv:2311.03309*, 2023.
- Yuan Yuan Wang, Wei Huang, Mingming Gong, Xi Geng, Tongliang Liu, Kun Zhang, and Dacheng Tao. Identifiability and asymptotics in learning homogeneous linear ode systems from discrete observations. *Journal of Machine Learning Research*, 25(154):1–50, 2024.
- Wes McKinney. Data Structures for Statistical Computing in Python. In Stéfan van der Walt and Jarrod Millman, editors, *Proceedings of the 9th Python in Science Conference*, pages 56 – 61, 2010. doi: 10.25080/Majora-92bf1922-00a.
- Xiaohua Xia and Claude H Moog. Identifiability of nonlinear systems with application to hiv/aids models. *IEEE transactions on automatic control*, 48(2):330–336, 2003.
- Shiyun Xu, Zhiqi Bu, Pratik Chaudhari, and Ian J Barnett. Sparse neural additive model: Interpretable deep learning with feature selection via group sparsity. In *Joint European Conference on Machine Learning and Knowledge Discovery in Databases*, pages 343–359. Springer, 2023.
- Andy B Yoo, Morris A Jette, and Mark Grondona. Slurm: Simple linux utility for resource management. In *Workshop on job scheduling strategies for parallel processing*, pages 44–60. Springer, 2003.

## A Theoretical results

### A.1 Proof of Lemma 2

**Lemma 2.** *A sparse-continuous random matrix with sparsity  $p$  is globally not identifiable with probability at least  $1 - (1 - p^n)^n - np^n(1 - p^n)^{n-1}$  for  $n \geq 2$  (and  $p$  for  $n = 1$ ).*

*Proof.* Following Theorem 1, the model Eq. (1) is globally unidentifiable if and only if  $A$  has more than one Jordan normal block for one of its eigenvalues, say  $\lambda_i$ , which then has geometric multiplicity  $g(\lambda_i) > 1$ , i.e.,  $\text{rank}(A - \lambda_i I) < n - 1$ . According to Lemma 1, it follows that  $P_A(\mathcal{U}) = P_A(\{A \in \mathbb{R}^{n \times n} \mid \text{rank}(A) < n - 1\})$ . Hence, we are looking for the probability of dependencies among columns in  $A$  that drop the rank. For a fixed zero structure  $B := (b_{i,j})_{i,j \in [n]} \in \{0, 1\}^{n \times n}$  the set on which  $X := (x_{i,j})_{i,j \in [n]} \in \mathbb{R}^{n \times n}$  introduces additional linear dependencies among the rows/columns of  $A$  has Lebesgue measure zero and thus zero probability under  $A$ . Therefore,  $P(\text{rank}(A) < n - 1) = P(\text{rank}(B) < n - 1)$ . We focus on the sufficient event that  $B$  has multiple zero columns. Since the entries of  $B$  are independent,  $P(B_{:,i} = 0) = p^n$  for all  $i \in [n]$  where  $B_{:,i}$  represents the  $i$ -th column, it follows that the random variable  $Z$  representing the count of zero columns follows a Binomial distribution  $Z \sim \text{Bin}(n, q)$  with  $q := p^n$ . With the probability mass function  $P(Z = k) = \binom{n}{k} q^k (1 - q)^{n-k}$  we find

$$P(\text{rank}(A) < n - 1) \geq P(Z \geq 2) = 1 - P(Z \in \{0, 1\}) = 1 - (1 - p^n)^n - np^n(1 - p^n)^{n-1}.$$

□

### A.2 Proof of Lemma 3

**Lemma 3** (sharp threshold for global unidentifiability). *Let  $A$  be a sparse-continuous matrix with  $n$ -dependent sparsity level  $p(n)$ . Then, for  $p_c(n) = 1 - \frac{\ln(n)}{n}$  and any function  $\omega(n) \rightarrow \infty$  we have the if  $p(n) = p_c(n) + \frac{\omega(n)}{n}$ , then  $P(\text{rank}(A) \leq n - 2) \rightarrow 1$  for  $n \rightarrow \infty$  and if  $p(n) = p_c(n) - \frac{\omega(n)}{n}$ , then  $P(\text{rank}(A) \leq n - 2) \rightarrow 0$  for  $n \rightarrow \infty$ . That is, there is a threshold at  $p = \ln(n)/n$  decisive for whether  $A$  is asymptotically globally unidentifiable with high probability or not.*

*Proof.* From  $A$  form the random bipartite graph  $G_{n,n,s}$  with  $A$  as the corresponding adjacency matrix. Edges are present independently with probability  $s = s(n) = 1 - p(n)$ .

For every bipartite graph  $G_{n,n,s}$  let

$$m(G) = \max\{|M| : M \text{ is a matching}\}, \quad d(G) = \max_{S \subseteq [n]} (|S| - |N(S)|) \quad (5)$$

(Hall deficiency). From Hall-König's theory for graph matching, the rank of the adjacency matrix  $A$

$$m(G) \leq \text{rank} A \leq n - d(G). \quad (6)$$

Given

$$s(n) = \frac{\ln n + \alpha(n)}{n},$$

we have that [Frieze and Karoński, 2015]  $P(m(G) = n) \rightarrow 1$  if  $\alpha(n) \rightarrow \infty$  and  $P(m(G) = n) \rightarrow 0$  if  $\alpha(n) \rightarrow -\infty$ .

*Case  $\alpha(n) \rightarrow -\infty$ .* Let  $Z$  be the number of isolated vertices in  $G_{n,n,s}$ . Without loss of generalization, we will consider isolated vertices from rows. Any fixed vertex is isolated with probability  $(1 - s)^n$  so

$$Z \sim \text{Bin}(n, (1 - s)^n), \quad \mathbb{E}[Z] = n(1 - s)^n = e^{-\alpha(n)}(1 + o(1)), \quad \text{Var}[Z] = O(\mathbb{E}[Z]).$$

Chebyshev's inequality therefore yields  $P(Z \geq 2) \rightarrow 1$  for  $n \rightarrow \infty$ . Two isolated vertices form a set  $S$  with  $|N(S)| \leq |S| - 2$ , so  $d(G) \geq 2$  and consequently  $\Pr[\text{rank} A \leq n - 2] \rightarrow 1$ .

*Case  $\alpha(n) \rightarrow +\infty$ .* Then  $P(m(G) = n) \rightarrow 1$ , hence  $P(\text{rank}(A) \leq n - 2) \rightarrow 0$ . Substituting  $s = 1 - p$  concludes the proof. □



### A.3 Proof of Lemma 4

**Lemma 4.** *Let  $A, A' \in \mathbb{R}^{n \times n}$  and assume there is an  $A$ -invariant subspace  $V^*$  such that  $(A - A')V^* = \{0\}$ . Then, for every  $t \geq 0$  and  $\mathbf{x}_0 \in \mathbb{R}^n$ , we have that*

$$\|e^{At}\mathbf{x}_0 - e^{A't}\mathbf{x}_0\|_2 \leq C(t, A, A')\|A - A'\|_2 d_A(\mathbf{x}_0)$$

with  $C(t, A, A') := \int_0^t \|e^{A(t-s)}\|_2 \|e^{A's}\|_2 ds$ . Further, for any  $\varepsilon > 0$ , the condition

$$\|(e^{At} - e^{A't})\mathbf{x}_0\| \leq \varepsilon \quad \text{for all } 0 \leq t \leq T$$

holds whenever

$$T \leq \frac{1}{\alpha} W\left(\alpha \frac{\varepsilon}{\|A - A'\| M^2 d_A(\mathbf{x}_0)}\right),$$

where  $W(\cdot)$  denotes the Lambert function and constants  $\alpha \in \mathbb{R}$ ,  $M \geq 1$  such that  $\|e^{At}\|, \|e^{A't}\| \leq Me^{\alpha t}$  for all  $t \geq 0$ .

*Proof.* Let us assume without loss of generality (otherwise we simply get a looser bound) that  $V^*$  is the closest proper  $A$ -invariant subspace to  $\mathbf{x}_0$ . We can then decompose  $\mathbf{x}_0$  as  $\mathbf{x}_0 = \Pi_{V^*}\mathbf{x}_0 + \mathbf{w}$  with  $\|\mathbf{w}\| = d_A(\mathbf{x}_0)$  (by definition, all norms are 2-norms). Given the assumption on  $A$  and  $A'$ , we have

$$(e^{At} - e^{A't})\mathbf{x}_0 = (e^{At} - e^{A't})(\Pi_{V^*}\mathbf{x}_0 + \mathbf{w}) = (e^{At} - e^{A't})\mathbf{w}.$$

From a variation of constants approach and the triangle inequality, we have

$$\|e^{At} - e^{A't}\| = \left\| \int_0^t e^{A(t-s)}(A - A')e^{A's} ds \right\| \leq \int_0^t \|e^{A(t-s)}\| \|e^{A's}\| \|A - A'\| ds,$$

which ultimately gives the result

$$\|e^{At}\mathbf{x}_0 - e^{A't}\mathbf{x}_0\| \leq \|e^{At} - e^{A't}\| \|\mathbf{w}\| \leq \|A - A'\| d_A(\mathbf{x}_0) \int_0^t \|e^{A(t-s)}\| \|e^{A's}\| ds.$$

For the second statement, we note that

$$\|(e^{At} - e^{A't})\mathbf{w}\| \leq \|A - A'\| M^2 \|\mathbf{w}\| \left( \int_0^t e^{\alpha s} ds \right) = \|A - A'\| M^2 d_A(\mathbf{x}_0) t e^{\alpha t},$$

which is bounded by  $\varepsilon$  for  $t \in [0, T]$  with

$$Te^{\alpha T} = \frac{\varepsilon}{\|A - A'\| M^2 d_A(\mathbf{x}_0)}.$$

Using the definition of the Lambert  $W$  function  $W(\cdot)$  we obtain

$$T = \frac{1}{\alpha} W\left(\alpha \frac{\varepsilon}{\|A - A'\| M^2 d_A(\mathbf{x}_0)}\right).$$

□

Assume  $A$  is identifiable from  $\mathbf{x}_0$ , but  $\mathbf{x}_0$  is close to a proper  $A$ -invariant subspace  $V^*$  with distance  $d_A(\mathbf{x}_0)$ . Then there exists another  $A' \neq A$  that agrees with  $A$  on  $V^*$ , i.e.,  $A'$  could practically be mistaken for the underlying true dynamic. Lemma 4 states that the trajectories under such  $A$  and  $A'$  indeed stay  $\varepsilon$ -close to each other up until time  $T$ .

## B Experimental details

### B.1 Software

We provide the resources with the corresponding licenses used in this work in Table 1.

Table 1: Overview of resources used in our work.

Name	Reference	License
Python	[van Rossum and Drake, 2009]	PSF License
PyTorch	[Paszke et al., 2019]	BSD-style license
Numpy	[Harris et al., 2020]	BSD-style license
Pandas	[pandas development team, 2020, Wes McKinney, 2010]	BSD-style license
Matplotlib	[Hunter, 2007]	modified PSF (BSD compatible)
Scikit-learn	[Pedregosa et al., 2011]	BSD 3-Clause
SciPy	[Virtanen et al., 2020]	BSD 3-Clause
SLURM	[Yoo et al., 2003]	modified GNU GPL v2
networkx	[Hagberg et al., 2008]	BSD 3-Clause
JAX	[Bradbury et al., 2018]	Apache-2.0

## B.2 Metrics

**System-level identifiability metrics.** To compute system level identifiability metrics, we perform a batched singular-value decomposition on every system matrix  $A$  using `jax.numpy.linalg.svd`. Subsequently, any singular value  $\sigma$  with  $|\sigma| < 10^{-6}$  is treated as numerically zero. Eigenvalues are computed with `jax.numpy.linalg.eigvals` and the matrix rank is computed via `jax.numpy.linalg.matrix_rank` with tolerance level set to  $10^{-6}$ .

**Trajectory-level identifiability metrics.** Smoothed condition number (SCN) analysis begins by constructing the empirical Gram matrix  $\hat{\Sigma}_{xx} = YSY^T \in \mathbb{R}^{d \times d}$ , where  $Y = [x(t_1) \dots x(t_n)]$  collects one simulated trajectory and where the diagonal “smoothing” matrix  $S$  contains the numerical quadrature weights (trapezoidal rule by default `jax.numpy.trapz`). The condition number is estimated with `jax.numpy.linalg.cond`.

**Normalized Hamming distance.** We use the normalized Hamming distance computed on binary input matrices to compare the true system matrix  $A$  with the empirically estimated matrix  $\hat{A}$ . To this end we first binarize  $A$  and  $\hat{A}$  via  $B = \mathbb{I}_\tau(A)$  and  $\hat{B} = \mathbb{I}_\tau(\hat{A})$  with threshold  $\tau = 10^{-5}$  and where  $\mathbb{I}_\tau$  is the indicator function that acts elementwise on matrix entries as

$$\mathbb{I}_\tau(a_{ij}) = \begin{cases} 1 & \text{if } a_{ij} > \tau; \\ 0 & \text{else} \end{cases}$$

The normalized Hamming distance between two matrices  $B, \hat{B} \in \mathbb{R}^{n \times n}$  is then defined as  $d_{\text{HMD}}(B, \hat{B}) = \frac{1}{n^2} \sum_{i,j} \mathbb{I}_{0.5}(B_{ij} \neq \hat{B}_{ij})$  where  $B_{ij} \neq \hat{B}_{ij}$  has to be understood as a boolean comparison which evaluates to one under equality and zero otherwise.

## B.3 Empirical estimators

**SINDy.** SINDy, short for Sparse Identification of Nonlinear Dynamics [Brunton et al., 2016], is a widely adopted algorithm for system identification. It leverages a user-defined set of basis functions to execute  $L_2$ -regularized linear regression, mapping observations of the solution trajectory  $\mathbf{x}(t_i)$  to their corresponding temporal derivatives  $\dot{\mathbf{x}}(t_i)$ . In practical applications, temporal derivatives are often unobservable, and SINDy estimates them through numerical finite difference approximations. We adopt the implementation available in PySINDy [de Silva et al., 2020], restrict the basis set to linear functions, and use the default optimization algorithm (sequentially thresholded least squares) which sets any coefficient whose magnitude falls below the user-defined threshold  $\lambda$  to zero. Model and optimizer come with several hyper-parameters out of which we tune the  $L_2$ -regularization strength ( $\alpha$ ), coefficient threshold ( $\lambda$ ), finite difference approximation order and maximum number of iterations separately for each sample.

**Regularization of SINDy.** For each trajectory we select the pruning threshold  $\lambda \in \{10^{-6}, \dots, 10^{-1}\}$  that enforces the sparsity gate: after every ridge-regression step any coefficient whose magnitude falls below  $\lambda$  is hard-set to zero, so increasing  $\lambda$  enforces progressively sparser candidate systems. Complementing this, the ridge weight  $\alpha \in \{0.001, 0.05, 0.1\}$  continuously shrinks the surviving coefficients toward the origin; larger values thus promote numerical stability

without directly changing the zero pattern. For every trajectory, we select the optimal parameters  $(\lambda, \alpha) = \operatorname{argmax} R^2$  where the  $R^2$  score is measured between the observed trajectory and the trajectory obtained by numerically solving the system estimate  $\hat{A}$  for the observed initial value. Finally, the identifiability analysis is based on systems with well-fitted trajectories only, which we define as trajectories for which the estimate achieves  $R^2 > 0.99$  and  $\text{MSE} < 10^{-4}$ .

**Neural ODEs.** Neural ODEs (NODEs) [Chen et al., 2018] use a parameterized function  $f_\theta(x(t))$  to approximate the dynamics underlying the observed trajectories. Instead of using finite difference schemes to estimate temporal derivatives, NODEs numerically integrate  $f_\theta$  to obtain a solution that can be directly compared to the observed trajectory. In practice  $f_\theta$  is implemented as a neural network; since we focus on linear systems, we use a model with multiple linear layers and no activation functions. To promote sparsity, we incorporate an L1 regularization term into the loss function. The total loss consists of the mean squared error (MSE) of the trajectories, augmented by the regularization parameter  $\lambda$  multiplied by the L1 norm of the network’s weights. To optimize the model we use the ode solvers implemented in torchode [Lienen and Günnemann, 2022], specifically the Dopri5 solver in combination with the IntegralController for adaptive step size selection, with relative and absolute tolerances set to  $1\text{e-}3$  and  $1\text{e-}6$ , respectively. Neural network parameters  $\theta$  are optimized with PyTorch’s RMSprop optimizer with a learning rate of  $1\text{e-}3$  to minimize the mean absolute error between the observed and predicted solution trajectory as in Chen et al. [2018]. Optimization proceeds for 10000 iterations or until the loss falls below  $10^{-5}$ .

**Sparsity-regularization of Neural ODEs.** For the LinearNODE experiments we first identify well-fitted trajectories which we define as trajectories for which the empirical estimate (after numerical integration from the ground truth initial value) achieves  $R^2 > 0.99$  or  $\text{MSE} < 10^{-4}$ . The proportion of well-fitted trajectories (among all trajectories) for different system dimensionalities  $n$  and sparsity levels  $p$  is displayed for different values of regularization weight  $\lambda \in \{0, 10^{-1}, 10^{-2}\}$  in Fig. 5. Among the  $\lambda$ -values that yield well-fitted trajectories, we then select the one that most faithfully reproduces the sparsity pattern of the ground-truth system matrix  $A$ . Specifically, for every trajectory we count the zero entries in the matrix estimate  $\hat{A}$  and in the true  $A$ , compute the absolute difference in these counts, and use this sparsity-mismatch score as our selection metric. The optimal  $\lambda$  for a given  $p$  is selected as the value that minimizes the average sparsity-mismatch across all well-fitted trajectories. The effect of regularization weight  $\lambda$ , system dimensionality  $n$  and sparsity  $p$  on the sparsity-mismatch between model estimate  $\hat{A}$  and ground truth system matrix  $A$  is illustrated in Fig. 6. Our arguably very permissive model selection strategy reflects the idea that we are only interested in

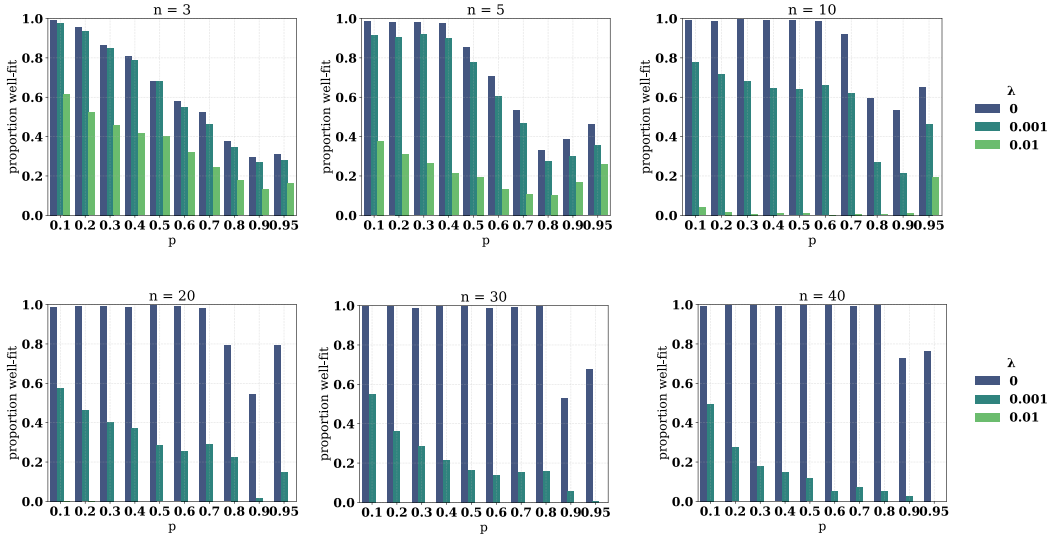


Figure 5: Proportion of trajectories that have been well-reconstructed by Sparse Neural ODEs for different regularization parameters  $\lambda$  and different dimensions  $n$  and sparsity levels  $p$ . For sparse systems, the model recovers only a smaller fraction of the trajectories.

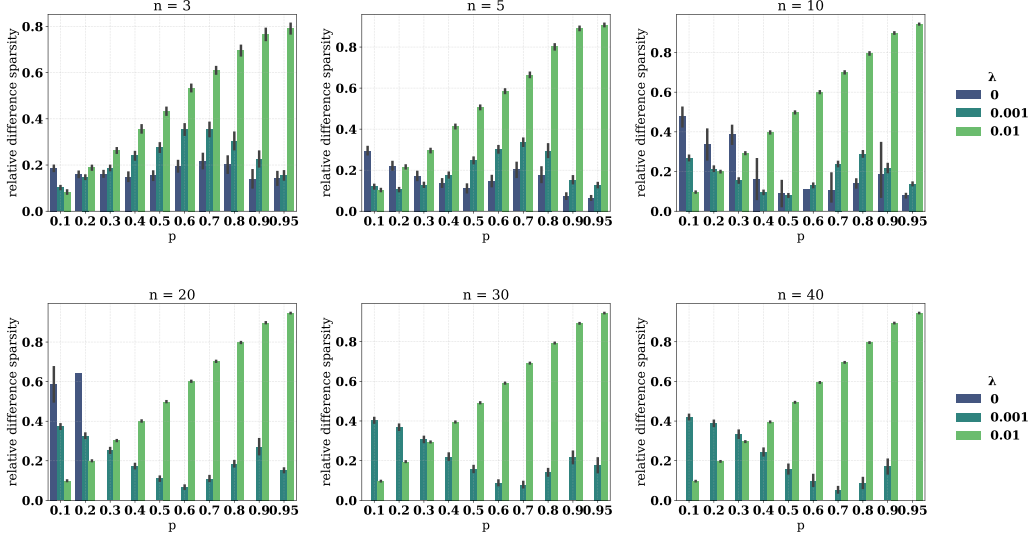


Figure 6: Relative difference in sparsity count (lower the better) between the true and reconstructed system matrices using Sparse Neural ODEs for different regularization parameters  $\lambda$  and different dimensions  $n$  and sparsity levels  $p$ . Lower regularization recovers dense matrices better, while higher values suit sparse ones.

well-fitted models (as measured on the trajectory-level) in order to draw conclusions about (empirical) system identifiability rather than about optimization, model architecture or numerical issues.

#### B.4 Additional results on trajectory-level identifiability metrics

We extend the results on trajectory-level identifiability metrics  $d_A$  and SCN to a broad range of system dimensions  $n$  and sparsity levels  $p$ . Box-plots for the two subgroups  $A_{\sigma_{2,\min}}$  and  $A_{\sigma_{2,\max}}$  introduced in Section 5.3 are displayed in Fig. 7 and Fig. 8. We observe the consistent trend that subgroup  $A_{\sigma_{2,\min}}$ , i.e., the subgroup with smaller second smallest singular value  $\sigma_2$ , leads to lower identifiability scores for both metrics (lower value for  $d_A$  and higher value for SCN) in line with our theoretical results.

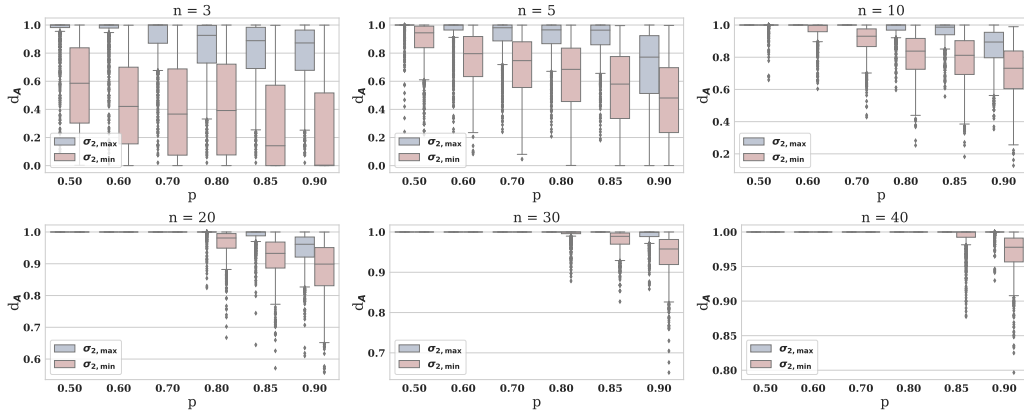


Figure 7: Box-plots of distance-to-unidentifiability  $d_A$  for the least and most identifiable groups of systems for different  $p$  and  $n$  values. Trajectories generated with  $A_{\sigma_{2,\min}}$  lead to smaller  $d_A$  than those produced with  $A_{\sigma_{2,\max}}$ .

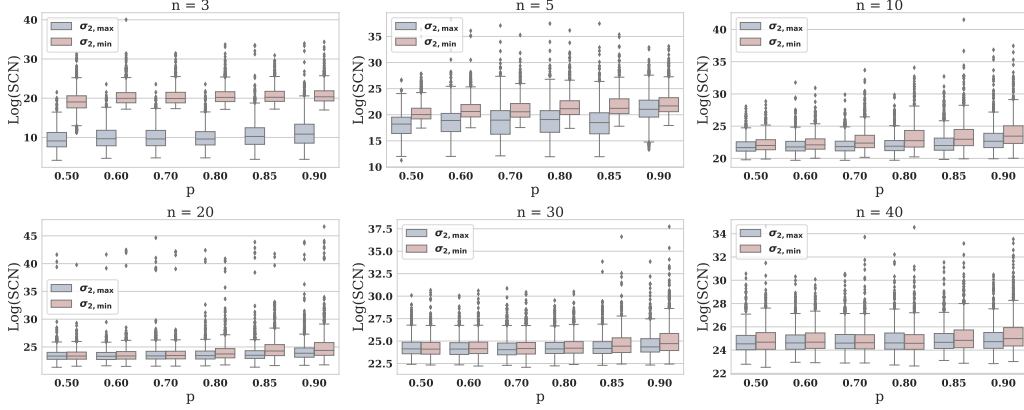


Figure 8: Box-plots of smoothed condition numbers (SCN) in log-scale for the least and most identifiable groups of systems for different  $p$  and  $n$  values. Trajectories generated with  $A_{\sigma_{2,\min}}$  lead to higher SCN than those produced with  $A_{\sigma_{2,\max}}$ .

**On the distance of a subspace of dimension  $n$  from a random vector on the unit sphere.** We now empirically validate the close-to-unidentifiability metric  $d_A$ , which measures the distance between an initial condition  $x_0$  and the kernel of the corresponding matrix  $A$ . Since we sample the initial conditions uniformly from the unit sphere, we can compare the empirical distribution of  $d_A$  to the theoretical expected distance between a random unit vector and a  $d_0$ -dimensional subspace of  $\mathbb{R}^n$ . We partition the trajectories by the null-space dimension  $d_0 = \dim(\ker(A))$  of their corresponding generating matrix  $A$  and display the resulting distance-to-unidentifiability  $d_A$  in Fig. 9. As expected, the (mean) empirical measure closely matches the theoretical expected distance between a random unit vector  $x_0$  and a  $d_0$ -dimensional subspace of  $\mathbb{R}^n$  [Vershynin, 2018], given by

$$\mathbb{E}[d_A(x_0) \mid n, d_0] = \frac{\Gamma(n/2)\Gamma((n - d_0 + 1)/2)}{\Gamma((n - d_0)/2)\Gamma((n + 1)/2)},$$

hence (in expectation) validating the computation of our distance-to-unidentifiability  $d_A$ .

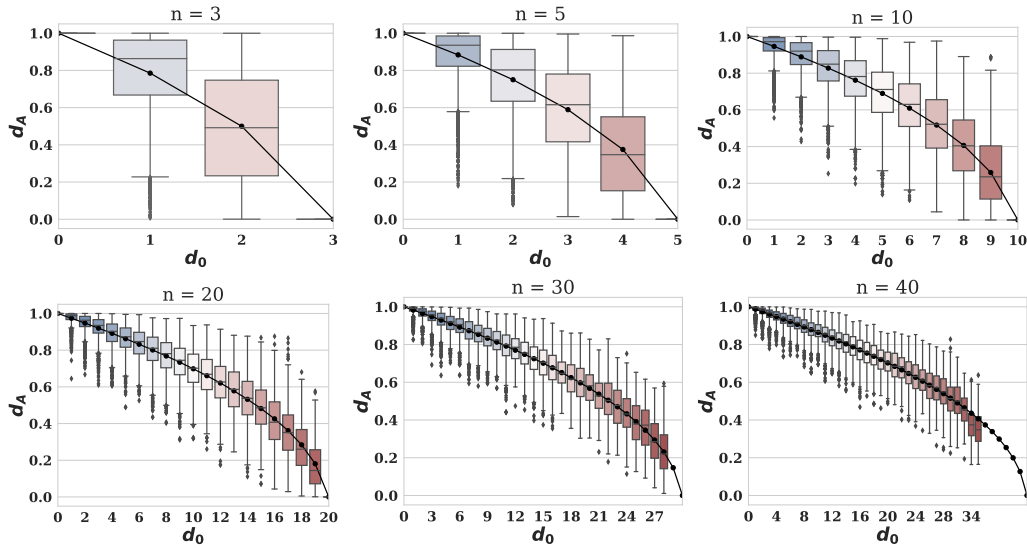


Figure 9: Box-plots of distance-to-unidentifiability  $d_A$  different  $n$  and different dimensions of  $\ker(A)$  ( $d_0 = \dim(\ker(A))$ ) together with the expected distance  $\mathbb{E}[d_A(x_0) \mid n, d_0]$  (black line).

## B.5 Extension to further matrix models

We focus on further random matrix models and present here the results.

**Fixed number of zeros per row ensemble.** In this random matrix model we fix the number of zeros per row such that each row contains exactly  $d(n) = \lfloor np \rfloor$  zeros. The remaining non-zero coefficients are sampled i.i.d. as  $a_{ij} \stackrel{iid}{\sim} N(0, 1)$ . We generate 100 system matrices and solve each of the for 100 initial values which are sampled uniformly at random from the unit circle in  $\mathbb{R}^n$ . Subsequently, we carry out the system-level identifiability and empirical identifiability analyses, following the same procedures described in the main text.

Results for both analyses are in line with the results reported in the main paper: system-level unidentifiability shows a sharp increase as sparsity increases (Fig. 10) and empirical identifiability shows a clear left-right gradient in Hamming distance for both SINDy (Fig. 13) and NODE (Fig. 14), confirming the expected rise in unidentifiability as sparsity increases.

**Sparse-Continuous ensemble with no zero rows or columns.** In this random matrix model we explicitly exclude matrices with zero rows or zero columns. For this, matrix entries are generated as  $a_{ij} = g_{ij}b_{ij}$ , where  $b_{ij} \stackrel{iid}{\sim} \text{Ber}(p)$  and  $g_{ij} \stackrel{iid}{\sim} N(0, 1)$ . We again attempt to generate 100 system matrices, however, not all dimensionality  $n$  and sparsity  $p$  combinations permit any system matrices with no zero rows or columns. (E.g. a  $3 \times 3$  matrix with sparsity level 0.9 will have  $\approx 8$  zeros and hence always multiple zero rows and/or columns.) We hence cap the number of attempts to generate a single matrix that fulfills the zero-rows / zero-columns constraints at 100 attempts. For every valid generated system matrix, we sample 100 initial values randomly from the unit circle in  $\mathbb{R}^\times$  and numerically solve the initial value problem to obtain 100 trajectories per system.

We perform system-level identifiability analysis as well as an empirical identifiability analysis. System-level metrics are provided in Fig. 11. Hamming-distances for different system dimensions  $n$  and sparsity levels  $p$  are reported in Fig. 13 for SINDy and in Fig. 14 for NODEs. For both estimators the average Hamming distance increases as sparsity rises, confirming the trends observed for other matrix models as well as the theoretical underpinnings.

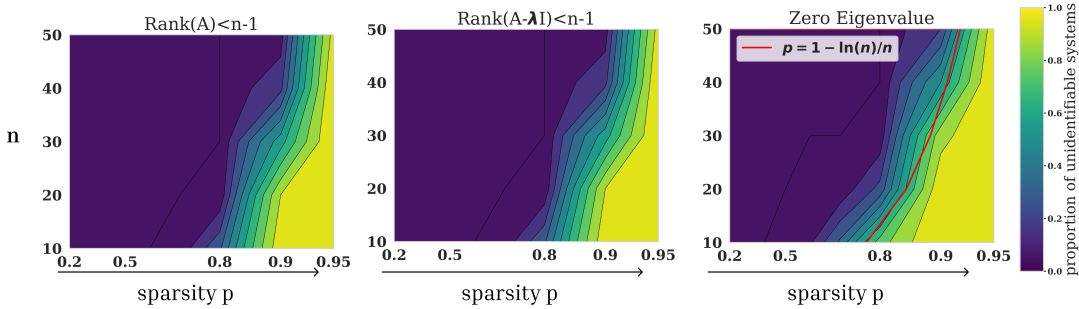


Figure 10: Proportion of matrices satisfying the conditions conditions  $\text{rank}(A - \lambda I) < n - 1$  (left),  $\exists \lambda \in \mathbb{R} : \text{rank}(A - \lambda I) < n - 1$  (center), and presence of zero eigenvalues (right) at different system dimensions  $n$  and sparsity levels  $p$  for **fixed number of zeros per row ensemble**.



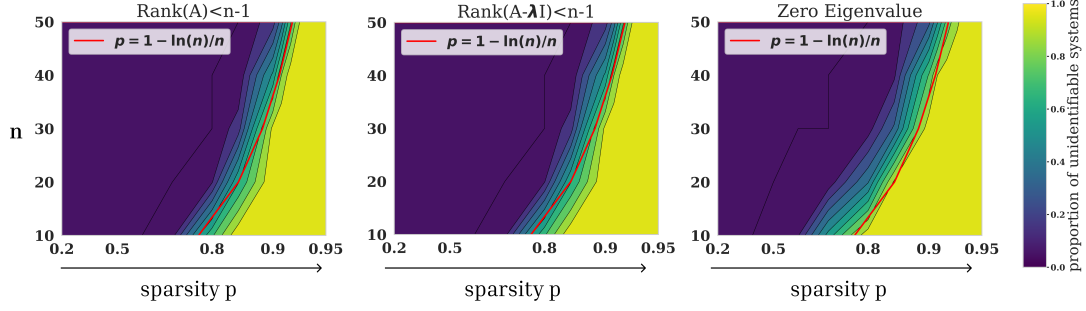


Figure 11: Proportion of matrices satisfying the conditions conditions  $\text{rank}(A - \lambda I) < n - 1$  (left),  $\exists \lambda \in \mathbb{R} : \text{rank}(A - \lambda I) < n - 1$  (center), and presence of zero eigenvalues (right) at different system dimensions  $n$  and sparsity levels  $p$  for **sparse-continuous ensemble with no zero rows**.

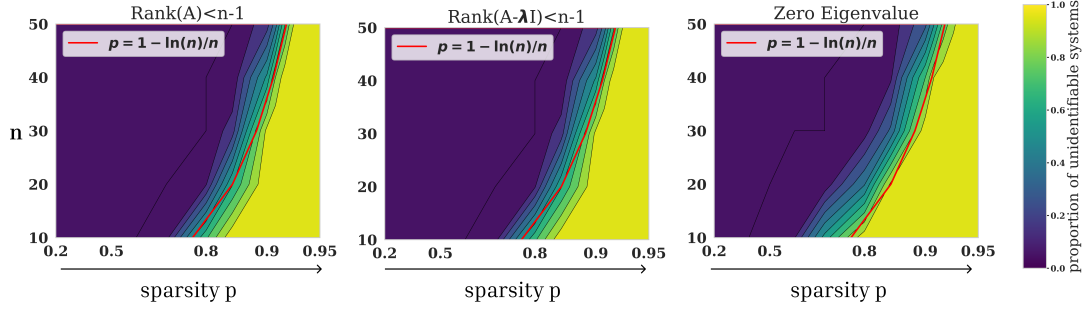


Figure 12: Proportion of matrices satisfying the conditions conditions  $\text{rank}(A - \lambda I) < n - 1$  (left),  $\exists \lambda \in \mathbb{R} : \text{rank}(A - \lambda I) < n - 1$  (center), and presence of zero eigenvalues (right) at different system dimensions  $n$  and sparsity levels  $p$  for **sparse-continuous ensemble with no zero columns**.

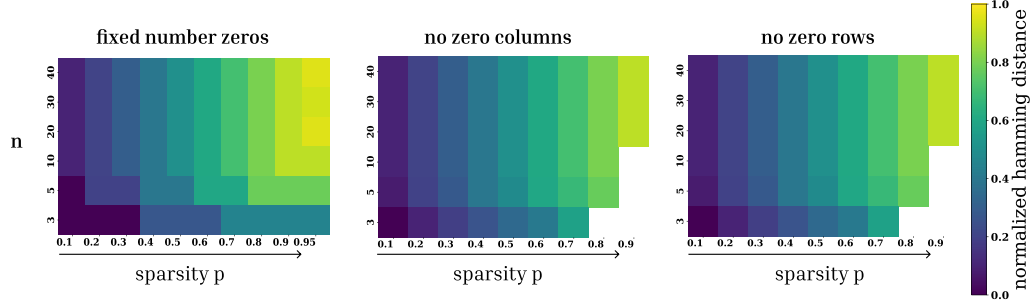


Figure 13: Hamming distance for different generating settings for SINDy on trajectories generated from **fixed number of zeros per row ensemble** (left), **sparse-continuous ensemble with no zero columns** (center), **sparse-continuous ensemble with no zero rows** (right).

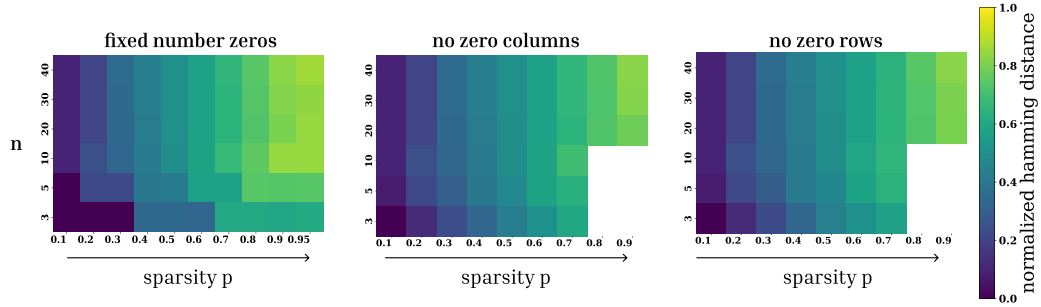


Figure 14: Hamming distance for different generating settings for NODE on trajectories generated from **fixed number of zeros per row ensemble** (left), **sparse-continuous ensemble with no zero columns** (center), **sparse-continuous ensemble with no zero rows** (right).